

## Supporting Information

# Revolutionizing energy storage with advanced reduced graphene oxide-wrapped MnSe@CoSe@FeSe<sub>2</sub> nanowires

Akbar Mohammadi Zardkhoshoui<sup>1\*</sup> and Saied Saeed Hosseiny Davarani<sup>2\*</sup>

<sup>1</sup>Department of Chemical Technologies, Iranian Research Organization for Science and Technology, Tehran 3313193685, Iran.

<sup>2</sup>Department of Chemistry, Shahid Beheshti University, G. C., 1983963113, Evin, Tehran, Iran.

Corresponding authors: \*<sup>1</sup>Tel: +98 21 56276283; Fax: +98 21 56276265; E-mail: A\_mohammadi@irost.ir (A. Mohammadi Zardkhoshoui) and \*<sup>2</sup>Tel: +98 21 22431661; Fax: +98 21 22431661; E-mail: [ss-hosseiny@sbu.ac.ir](mailto:ss-hosseiny@sbu.ac.ir) (S.S.H. Davarani).

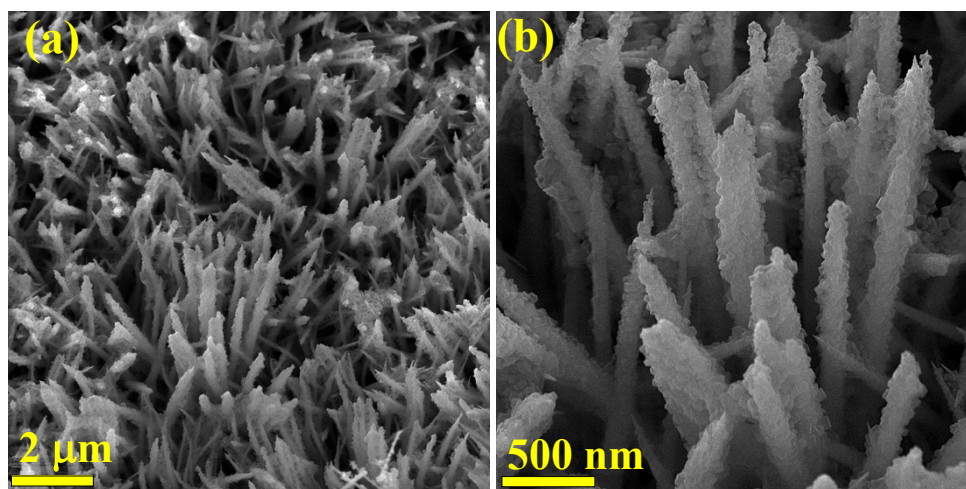


**Fig. S1** (a, b) FESEM images of the NF@MCFS300.

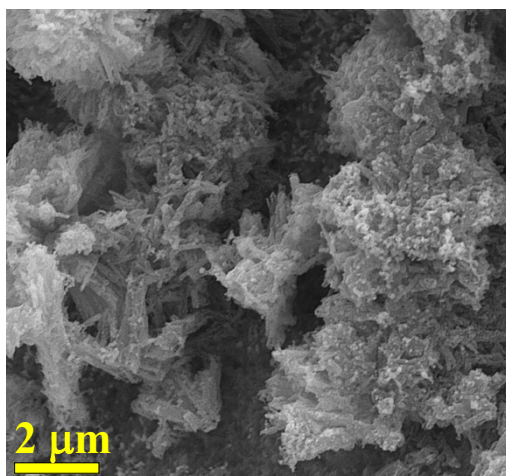


Fig. S2 FESEM images of the NF@MCFS600.

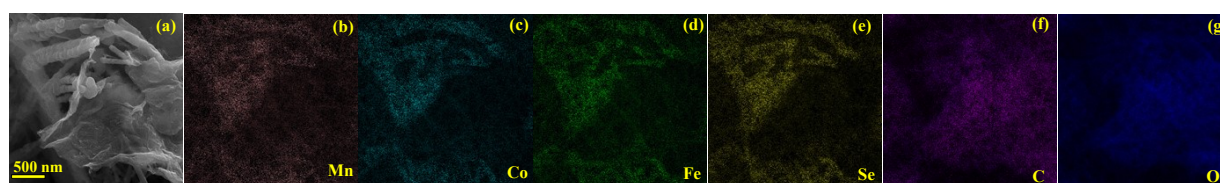


Fig. S3 FESEM mapping images of the NF@MCFS500-rGO.

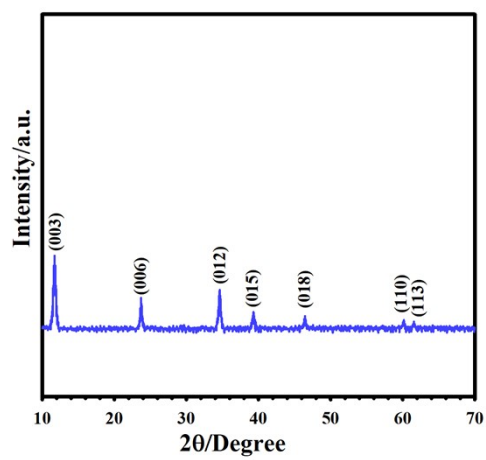


Fig. S4 XRD pattern of the MCFLDH.

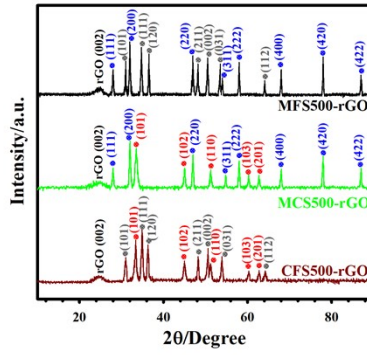


Fig. S5 XRD patterns of the MFS500-rGO, CFS500-rGO, and MCS500-rGO.

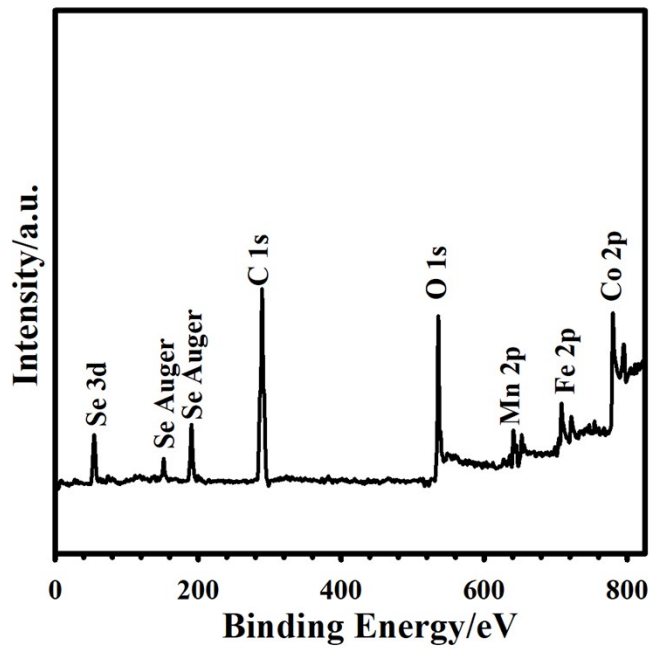
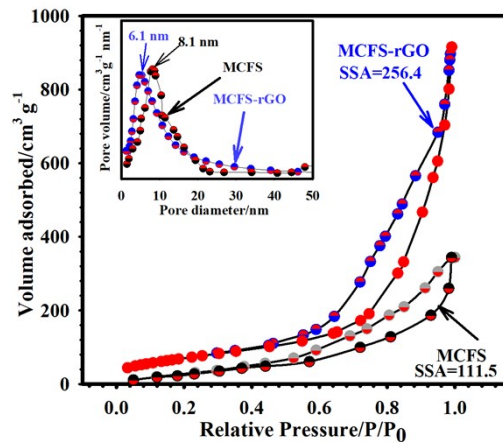
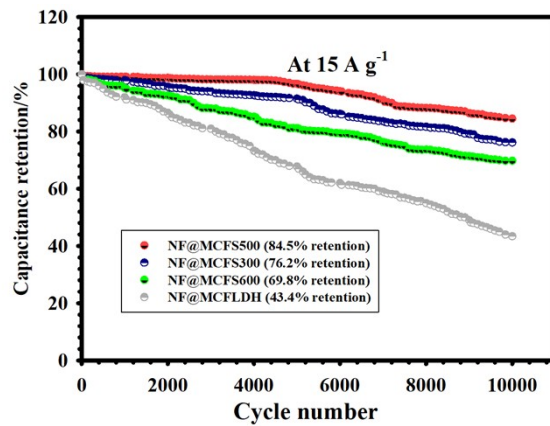


Fig. S6 Comprehensive XPS profile of the MCFS500-rGO.



**Fig. S7** BET graphs of the MCFS500-rGO and MCFS500 along with their corresponding BJH graphs (inset).



**Fig. S8** Longevity of the NF@MCFLDH, NF@MCFS300, NF@MCFS500, and NF@MCFS600 electrodes at 15 A g<sup>-1</sup>.

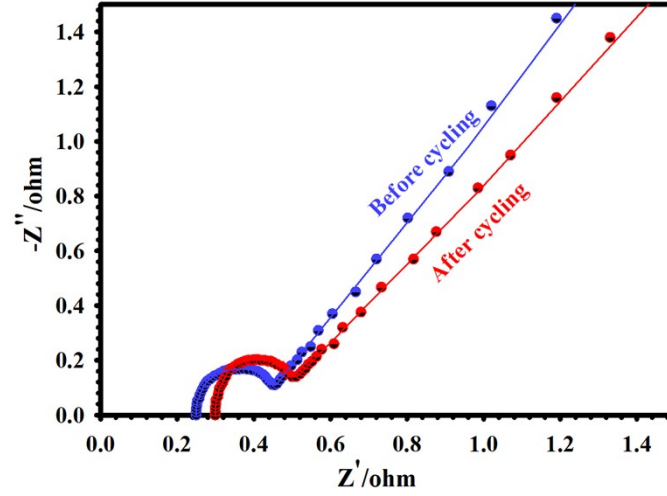


Fig. S9 EIS curves of the NF@MCFS500-rGO before and after 10000 cycles.

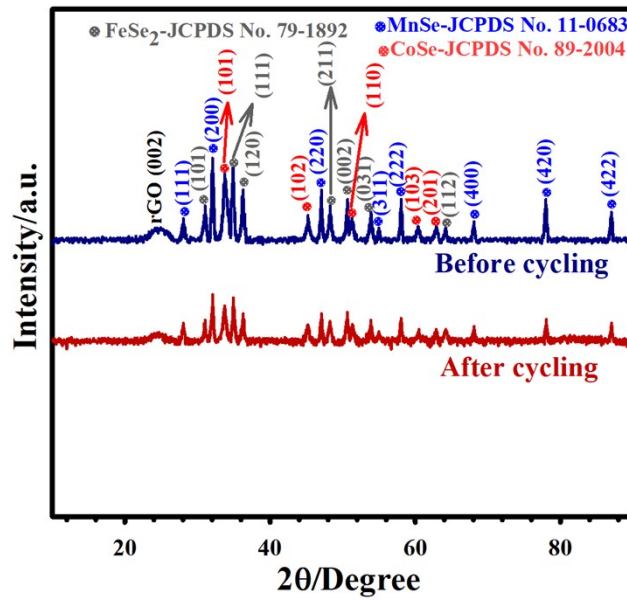
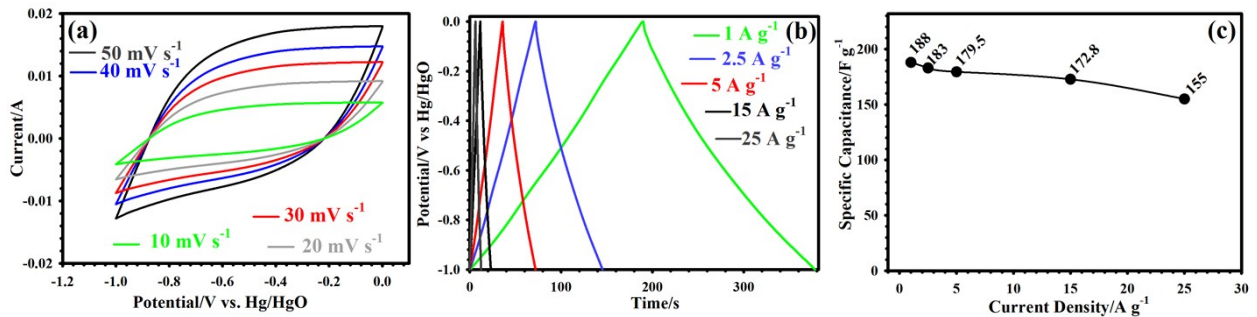
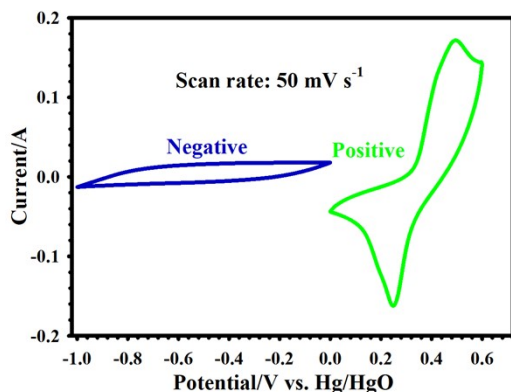


Fig. S10 XRD pattern of the MCFS500-rGO before and after 10000 GCD cycles.



**Fig. S11** (a) CV plots of the AC from 10 to 50 mV s<sup>-1</sup>. (b) GCD plots of the AC from 1 to 25 A g<sup>-1</sup>. (c) Rate capability of the AC electrode.



**Fig S. 12** CV plots of AC (negative electrode) and NF@MCFS500-rGO (positive electrode) at 50 mV s<sup>-1</sup> in three-electrode cell.

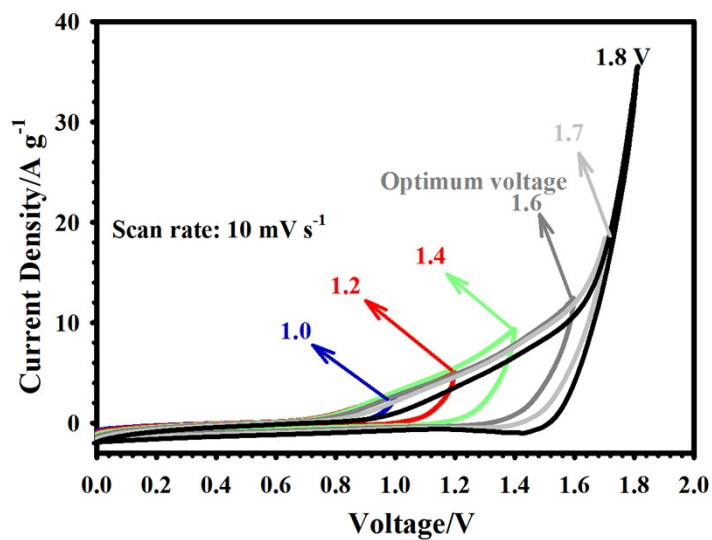


**Fig. S13** CV plots of the AC/NF@MCFS500-rGO at various potential window at 10 mV s<sup>-1</sup> from 1.0 to 1.8 V.

**Table S1.** Comparison of the supercapacitive performance of the NF@MCFS500-rGO with other

Composition	Capacitance (F/g)	Cycles, retention	Rate capability	ED (Wh kg <sup>-1</sup> )	Reference
NiSe-Ni <sub>0.85</sub> Se	1486.6 at 1 A g <sup>-1</sup>	5000, 80%	69% at 20 A g <sup>-1</sup>	41	1
CuSe@MnSe	1270.6 at 1 A g <sup>-1</sup>	7000, 91.62%	60.3% at 30 A g <sup>-1</sup>	19.54	2
Sn-Co(OH) <sub>2</sub>	1441.8 at 1 A g <sup>-1</sup>	5000, 84.3%	49.5% at 5 A g <sup>-1</sup>	-	3
NiCoP/Co(OH) <sub>2</sub>	1604 at 1 A g <sup>-1</sup>	5000, 91.1%	81.8% at 20 A g <sup>-1</sup>	38.4	4
Ni <sub>0.85</sub> Se	1354 at 1 A g <sup>-1</sup>	300, 90%	49.55% at 30 A g <sup>-1</sup>	40.7	5
MnCo <sub>2</sub> O <sub>4</sub> /MnO <sub>2</sub>	1539 at 1 A g <sup>-1</sup>	10000, 95.5 %	51.2% at 20 A g <sup>-1</sup>	48.78	6
CoSe <sub>2</sub> /NC-NF	1236.5 at 1 A g <sup>-1</sup>	10000, 92%	61.2% at 20 A g <sup>-1</sup>	40.9	7
Cerium Selenide	451.4 at 1 A g <sup>-1</sup>	4000, 70.7%	65% at 15 A g <sup>-1</sup>	36.1	8
Co <sub>x</sub> Ni <sub>1-x</sub> Se	918.8 at 1 A g <sup>-1</sup>	4000, 83.9%	47% at 10 A g <sup>-1</sup>	-	9
3DG/ZnSe-SnSe <sub>2</sub>	1515.2 at 1 A g <sup>-1</sup>	3000, 90.1% (3 E)	64.5% at 20 A g <sup>-1</sup>	25.3	10
MnCo <sub>2</sub> O <sub>4</sub> @MoS <sub>2</sub>	512 at 1 A g <sup>-1</sup>	5000, 99.57% (3 E)		36	11
NiCo <sub>2</sub> S <sub>4</sub> @DCCNF)	1474 at 1 A g <sup>-1</sup>	5000, 90.2% (3 E)	80% at 20 A g <sup>-1</sup>	55.6	12
NF@MCFS-rGO	1830 at 1 A g <sup>-1</sup>	10000, 93.25% (3 E)	78.5% at 25 A g <sup>-1</sup>	64.6	This work

previously reported selenide based-electrodes.

## References

1 Y. Bai, W. Shen, K. Song, S. Zhang, Y. Wang, T. Xu, J. Xu, S. Dai and X. Wang, *J. Electroanal. Chem.*, 2021, **880**, 114795.

- 2 G. Tang, X. Zhang, B. Tian, P. Guo, J. Liang and W. Wu, *Chem. Eng. J.*, 2023, **471**, 144590.
- 3 G. Nabi, A. Riaz, A. Dahshan, M. Tanveer, M. Maraj and W. Ali, *Mater. Chem. Phys.* Volume 2024, 314, n128944.
- 4 R. Xie, S. Liu, Y. Rao, A. Karim, X. Qi, H. Huang and H. Xuan, *J. Alloys Compd.* 2023, 969, 172368.
- 5 S. Wang and S. Ma, *Dalton Trans.*, 2019, **48**, 3906–3913.
- 6 M, Manigandan and P. R. Vanga, *J. Energy Storage* 2024, **100**, 113783.
- 7 C. Miao, X. Xiao, Y. Gong, K. Zhu, K. Cheng, K. Ye, J. Yan, D. Cao, G. Wang and P. Xu, *ACS Appl. Mater. Interfaces*, 2020, **12**, 9365–9375.
- 8 B. Pandit and B. R. Sankapal, *ACS Appl. Nano Mater.* 2022, **5**, 3007–3017.
- 9 X. Liu, D. Zhang, Y. Ma, G. Li, X. Yuan, Y. Huang, G. Liu, M. Guo and W. Zheng, *ACS Appl. Nano Mater.* 2024, **7**, 8880–8889.
- 10 T. Zhao, G. Feng, L. Zhou, X. Wang, X. Li, F. Jiang, H. Li, Y. Liu, Q. Yu, H. Cao, Y. Xu and Y. Zhu, *ACS Appl. Nano Mater.* 2024, **7**, 13434–13446.
- 11 P. S. Shukla, A. Agrawal, A. Gaur and G. D. Varma, *J. Energy Storage* 2023, 59, 106580.
- 12 Y. Xiao, J. Huang, Y. Xu, H. Zhu, K. Yuan and Y. Chen, *J. Mater. Chem. A*, 2018, **6**, 9161-9171.